

# Electrochemical Behavior of Polyaniline-Modified Cation-Exchange Heterogeneous Membranes in Solutions Containing Mono- and Bivalent Cations

M. A. Brovkina<sup>a, \*</sup>, N. A. Kutenko<sup>a</sup>, and N. V. Loza<sup>a</sup>

<sup>a</sup> Kuban State University, Krasnodar, 350040 Russia

\*e-mail: andreeva\_marina\_90@bk.ru

Received January 13, 2023; revised January 28, 2023; accepted February 7, 2023

**Abstract**—A series of composite ion-exchange membranes based on an heterogeneous cation-exchange MK-40 membrane and polyaniline is obtained under the conditions of electrodiffusion of a monomer and an oxidizing agent. The process of polyaniline synthesis on the membrane surface is accompanied by recording of chronopotentiograms and pH of the solution leaving the desalination compartment. The initial cation-exchange MK-40 membrane and obtained composites based on it are studied by voltammetry and chronopotentiometry in solutions of NaCl, CaCl<sub>2</sub>, and MgCl<sub>2</sub> in the same flow-type electro dialysis cell, in which the composites are obtained. To calculate the transport numbers of counterions in the membranes in solutions of CaCl<sub>2</sub> and MgCl<sub>2</sub> by chronopotentiometry, the apparent fraction of the conductive membrane surface in a solution of NaCl is calculated based on the experimental data on the potentiometric transport numbers of counterions in the membrane. The conditions for the synthesis of polyaniline on the surface of an heterogeneous MK-40 membrane which result in the preparation of samples with selectivity to singly charged ions are found out.

**Keywords:** ion-exchange membrane, polyaniline, modification, current–voltage curve, chronopotentiogram, transport numbers

**DOI:** 10.1134/S2517751623030034

## INTRODUCTION

Growing demand for agricultural and industrial products determined by fast population growth leads to one of the inevitable global problems—fresh water shortage [1, 2]. According to the calculations of researchers, the amount of required water will become smaller than the pace of growth in its consumption by about 2050. Salt water accounts for 97.5% of the total water resources on the Earth, while fresh water occupies just 2.5%. Here, 97% of it is concentrated in the polar ice. Because of this, implementation of possible programs on the recovery of the water resources of the planet needs the use of highly efficient technologies of desalination of sea and brackish water.

Thermal (based on a change in the phase state) and membrane (take place without a change in the phase state) processes of water desalination are distinguished [2]. Membrane processes are more effective and less energy-consuming in comparison with thermal processes [3, 4]. Membrane processes include direct and reverse osmosis, pervaporation, membrane distillation, electrodialysis, etc. [5]. Among them, reverse osmosis is the leading method due to the systematic decrease in power consumption from 20 down to 2.5 kWh for the production of a cubic meter of fresh

water [1]. The advantages of this method are low operational costs, simplicity of the module design, and low power consumption. However, the concentrate left after reverse osmosis can contain moderate and high concentrations of inorganic and/or organic compounds. The problem of disposal of the concentrate formed in the process of desalination of sea and brackish water acquires a global scale. If the concentrate is directly discharged into sea water, the ecosystem is endangered [6]. From the environmental standpoint, the attention of researchers should be focused at finding out and developing possible technologies for alleviating the potential impact of the concentrate on the environment.

By today, electrodialysis is an economically sound and available method of disposal of the concentrate formed after the application of reverse osmosis. It makes it possible to extract for reuse over 90% water and provide discharges with a zero level of contamination [7–9]. However, one of the substantial problems limiting wide application of electrodialysis is concentration polarization that appears at membrane/solution boundaries and leads to deposit formation due to the increase in the concentration of hydroxyl ions. The problem of formation of deposits of low-soluble salts is

one of the disadvantages of the application of this method. Since the deposit is mainly formed from the side of the concentration compartment, decreasing the concentration of cations capable of deposit formation in it could have decreased this negative effect. The application of ion-exchange membranes selective to singly charged ions helps overcoming the problem of deposit formation and increasing selective isolation of ions of a certain kind.

The mechanism of selective separation of ions can be explained by one of the effects considered below [10]. First, by a sieve effect determined by the steric factor: the size of the pores of the membranes and difference in the radii of ions in the hydrated state. By increasing the crosslinking of the ion-exchange component, it is possible to increase the transport of ions with a smaller radius in the hydrated state through the membrane [11]. Varying the concentration of the crosslinking agent makes it possible to optimize the pore size for the appearance of a sieve effect in relation to the required ions. Second, by an electrostatic barrier induced by stronger repulsion of doubly charged ions in comparison with singly charged ions [12]. Preparation of a membrane selective to singly charged ions can be achieved by modifying the surface of the membrane with a layer that has an opposite sign of the charge of the fixed groups relative to the initial membrane. The methods of surface modification are divided to physicochemical and covalent chemical [10]. As opposed to covalent chemical modification, physicochemical modification does not lead to the formation of covalent bonds. The modified layer is held on the membrane due to electrostatic attraction and intermolecular forces. Physicochemical modification includes surface polymerization, direct application of a modifier, its electrodeposition, and layer-by-layer self-assembly [10]. Pyrrole [13], aniline [14], dopamine [15], etc. are used as a monomer for the surface modification of membranes. The obtained dense layer of a polymer on the surface of a membrane repulses ions with a higher charge. Third, by the difference in the Gibbs hydration energy of ions [16]. For this, e.g., the hydrophilic–hydrophobic balance of the membrane surface is changed during modification. Therefore, a barrier for the passage of a hydrated ion through the hydrophobic layer on the membrane surface is created. Ions with a lower hydration energy have a weak bond with water molecules, because of which it is easier for them to pass through a membrane pore.

Polyaniline (PANi) is one of the promising modifiers that make it possible to solve the problem of selective separation of singly and doubly charged ions. A thin anion-exchange layer of PANi on the surface of a cation-exchange membrane to a greater extent repulses multiply charged ions in comparison with singly charged ions due to the presence of positively charged nitrogen-containing centers [17–19].

An important task is the assessment of the selectivity of ion-exchange membranes, a quantitative characteristic of which is transport numbers (TNs) of counterions in a membrane. There are various approaches to their determination. The most common method is the determination of TNs from the value of the membrane potential measured under the conditions when a membrane separates two solutions of the same electrolyte with its different concentrations [20]. An advantage of the method is the simplicity of its implementation, while an apparent disadvantage is the uncertainty of the value of the concentration of the electrolyte, to which the found value should be normalized. Another approach to the estimation of TNs is their experimental determination by the Hittorf method [21]. However, the results of determination of TNs by this method will be greatly affected by the experiment conditions as well as auxiliary membranes surrounding the membrane under study. The TNs of counterions in a membrane can be calculated within the framework of a microheterogeneous membrane based on the results of the measurement of the concentration dependences of the specific electrical conductivity and diffusion permeability of membranes [22]. However, this requires executing a copious amount of experimental work. Another method of determination of TNs is based on the sharing of results of chronopotentiometry and the Sand equation [23]:

$$\tau_{\text{Sand}} = \frac{\pi D}{4} \left( \frac{zF}{\bar{t}_c - t_c} \right)^2 \left( \frac{C_0}{i} \right)^2, \quad (1)$$

where  $\tau_{\text{Sand}}$  is the transition time at the current density  $i$ ;  $D$  and  $C_0$  are the coefficient of diffusion and concentration of the electrolyte, respectively;  $z$  is the charge of the counterion; and  $\bar{t}_c$  and  $t_c$  are the transport numbers of the cations in the membrane and solution, respectively. In the case of a homogeneous membrane,  $\tau_{\text{Sand}}$  can be determined from the chronopotentiogram. After that, having plotted the graph of the dependence of  $\tau_{\text{Sand}}$  on  $(C_0^2/i^2)$ ,  $\bar{t}_c$  can be calculated. However, in the case of a heterogeneous membrane, the nonuniformity of the conductivity of its surface should be taken into account. For this, Choi and Moon [24] introduced an apparent fraction of the working surface of a membrane  $\varepsilon$  into the Sand equation, which makes it possible to determine the TNs of ions in a heterogeneous membrane:

$$\tau = \varepsilon^2 \frac{\pi D}{4} \left( \frac{zF}{\bar{t}_c - t_c} \right)^2 \left( \frac{C_0}{i} \right)^2, \quad (2)$$

where  $\tau$  is the transition time experimentally determined from the chronopotentiogram of a heterogeneous membrane at the corresponding current density.

It should be noted that the applicability of the Sand equation is determined by the value of the current density, thickness of the diffusion layer, and nonuniformity

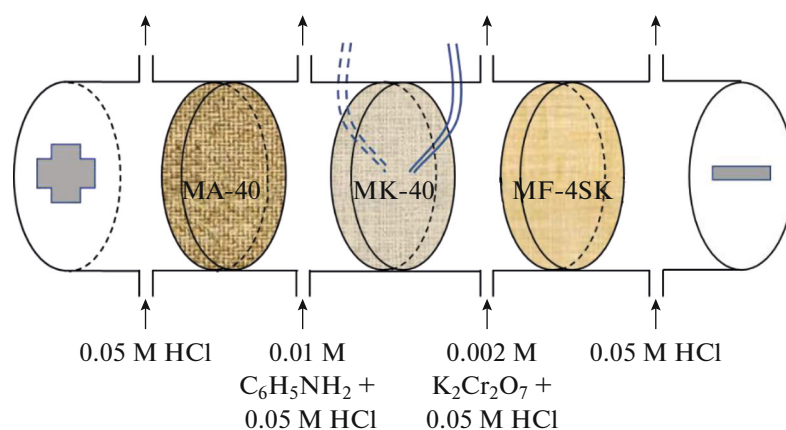


Fig. 1. Four-compartment cell for the preparation of composites and measurement of CVCs and ChPs.

mity of the surface [25]. Also, the theory of Choi and Moon supposes the presence of the normal component of the electric current only, while the tangential component is neglected [25]. Therefore, having determined the apparent fraction of the conductive surface by chronopotentiometry in solutions of NaCl or KCl, this value can be used for the calculations of TNs in other solutions because it is apparent that it does not depend on the nature of the solution but is only determined by the microstructure of the surface. However, the determination of the apparent fraction of the surface by Eq. (2) requires the values of the TNs of the ions in the membrane found by an independent method, and they can be determined by any of the above methods.

The aim of this work is to study the effect of aniline polymerization time in a commercial heterogeneous cation-exchange MK-40 membrane under the conditions of electrodiffusion of a monomer and an oxidizing agent at underlimiting current modes on the electrochemical behavior of modified membranes to increase their specific selectivity to singly charged cations.

## EXPERIMENTAL

### Membranes

A heterogeneous cation-exchange MK-40 membrane (OOO Shchekinoazot) was used as the initial membrane. The membrane consists of a mixture of polyethylene, a Capron reinforcing cloth, and 65% strongly acidic sulfo cation exchanger obtained by sulfonation of styrene–divinylbenzene copolymer [26]. All the composite membranes were obtained based on an MK-40 membrane.

A anion-exchange MA-40 membrane and a cation-exchange MF-4SK membrane were used as auxiliary membranes in the preparation of the composites and measurements of the current–voltage curves (CVCs) as well as chronopotentiograms (ChPs). An MA-40 membrane contains polyethylene, a Capron reinforcing

cloth, and 55% polyfunctional anion exchanger containing quaternary ammonium bases and secondary and tertiary amines [26]. An MF-4SK membrane is a homogeneous film made of perfluorinated sulfo-containing polymer which is similar to a Nafion membrane.

### Preparation of Composite Membranes

The synthesis of polyaniline (PANi) on the surface of an MK-40 membrane described in [27] was executed in a four-compartment electrodiffusion cell under the conditions of electrodiffusion of a monomer and an oxidizing agent (Fig. 1). A 0.01 M solution of aniline in 0.05 M hydrochloric acid was used as the monomer and a 0.002 M solution of potassium dichromate in 0.05 M hydrochloric acid was used as the oxidizing agent. A 0.05 M solution of hydrochloric acid circulated in the near-electrode compartments. Direct electric current was supplied to platinum polarizing electrodes. However, as opposed to the earlier performed works, the current density was a half of the limiting current density  $i_{lim}$  of the initial MK-40 membrane to minimize the contribution from the conjugate effects of concentration polarization during the synthesis of PANi. The value of  $i_{lim}$  of an MK-40 membrane was determined by the tangent method by the data of CVCs in a 0.05 M solution of HCl. The polarizable surface of the membranes was 7.1 cm<sup>2</sup>. The speed of circulation of the solution was 15 mL/min. The membrane potential  $\phi$  was measured using silver/silver chloride electrodes connected to capillaries brought to the surface of the membrane under study from two sides to control the process of synthesis. The time of synthesis of PANi was 90, 180, and 300 min. The experiments were accompanied by the recording of pH of the solution leaving the desalination compartment.

The concentration of aniline in the solution before and after the synthesis of PANi was determined by a

photometric method based on the interaction of aniline with *p*-dimethylaminobenzaldehyde [28] at a wavelength of 432 nm.

#### Electrochemical Behavior of Membranes

The CVCs and ChPs of the initial and composite membranes were studied in the same four-compartment electro dialysis cell, in which the composites were prepared. A 0.05 M solution of NaCl circulated in the near-electrode compartments. A solution of one of the electrolytes, NaCl, MgCl<sub>2</sub>, or CaCl<sub>2</sub>, the concentration of which was 0.05 mol-equiv/L, was fed to the compartments located on both sides of the membrane under study. The CVCs were measured at different speeds of circulation of the solution through all the compartments which varied from 14 up to 50 mL/min. When measuring the ChPs, the flow rate of the solutions was 14 mL/min. All the experiments were accompanied by the recording of pH of the solution leaving the desalination compartment.

#### Determination of Transport Numbers of Ions in the Membrane by a Potentiometry

The membranes under study were preliminarily equilibrated with a 0.03 M solution of NaCl. Then the membrane under study was placed into a two-compartment cell, the compartments of which were filled with 0.03 M and 0.06 M solutions of NaCl (Fig. 2). Silver/silver chloride electrodes were placed into the compartments of the cell on both sides of the membrane under study, through which solutions circulated at a rate of 350 mL/min. The value of the electromotive force (EMF)  $\Delta E_{\text{exp}}$  was recorded every 5 min until reaching a steady state. To exclude an error associated with the presence of asymmetry potentials in the measuring electrodes, the experiment was performed at different polarities of the measuring electrodes. The average value of the EMF from five measurements was used in the calculations.

The potentiometric transport numbers of counterions  $t_i^{\text{app}}$  were calculated by the formula

$$t_i^{\text{app}} = \frac{\Delta E_{\text{exp}}}{\Delta E_{\text{theor}}}, \quad (3)$$

where  $\Delta E_{\text{theor}}$  is the EMF of a cell with an ideally selective membrane calculated by the formula

$$\Delta E_{\text{theor}} = \frac{RT}{F} \ln \frac{(m\gamma_{\pm})_1}{(m\gamma_{\pm})_2},$$

where  $R$  is the gas constant,  $T$  is the temperature,  $F$  is the Faraday constant,  $m$  is the molal concentration of the solution, and  $\gamma_{\pm}$  is the mean activity coefficient of the solution [29].

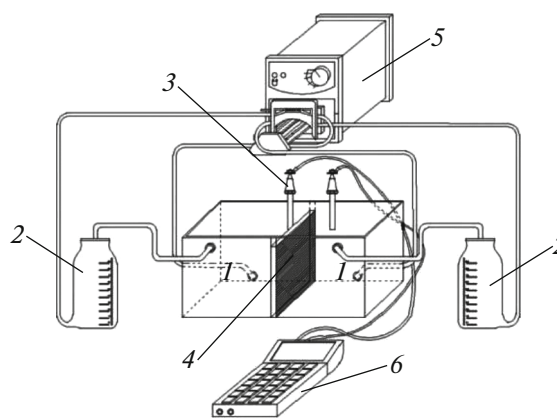


Fig. 2. Unit for the measurement of the potentiometric transport numbers of counterions in the ion-exchange membrane: (1) compartments of the measuring cell, (2) vessels for solutions, (3) measuring silver/silver chloride electrodes, (4) a membrane, (5) a peristaltic pump, and (6) an ionometer.

#### Measurement of ChPs and Determination of Transport Numbers of Ions in the Membrane Based on Them

ChPs were measured in the same four-compartment electro dialysis cell, in which the composites were obtained. The measurements were performed in three different solutions: NaCl, CaCl<sub>2</sub>, and MgCl<sub>2</sub> with a concentration of 0.05 mol-equiv/L. The membrane under study was in a horizontal position, and the desalination compartment was under the concentration compartment. Therefore, the appearance of natural convection was minimized. During the measurement, the solution was not pumped through the cell, there was no forced convection. Current with the intensity of 10 up to 50 mA was fed to platinum polarizing electrodes. To calculate the transport numbers of counterions through the (2) was used.

#### Physicochemical Characteristics of Membranes

The thickness of the membrane was measured by an MK 0-25 micrometer (model 102, Russia) at least 10 times, after which the obtained values were averaged and confidence intervals were calculated.

The water content in the ion-exchange membranes was determined by a method of air heat dehydration at 70–80°C. The weight fraction of water in the membrane in percents was calculated by the formula

$$W = \frac{m_{\text{sw}} - m_{\text{dr}}}{m_{\text{sw}}},$$

where  $m_{\text{sw}}$  is the weight of the swelled membrane, g, and  $m_{\text{dr}}$  is the weight of the dry membrane, g.

The surfaces of the swelled composite membranes were visualized using an Altami BIO-2 optical microscope equipped with a UCMOSO5100KPA digital ocular USB camera (magnifications of 4×, 10×, 40×).

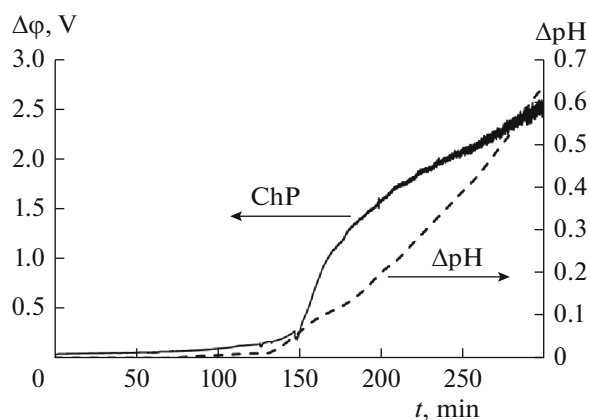


**Fig. 3.** ChP measured during the synthesis of PANi and corresponding changes in pH of the solution leaving the desalination compartment.

## RESULTS AND DISCUSSION

### Preparation of the Composite Membranes

Figure 3 presents the ChP recorded in the process of preparation of a composite based on an MK-40 membrane and polyaniline (MK-40/PANi) for 5 h. Also, the change in pH of the solution leaving the desalination compartment was recorded during the experiment. During the first 2 h of modification, the shape of the ChP corresponds to the classical shape for binary electrolytes at currents below the limiting current [23]. At the moment of current supply, immediate drop in the difference of potentials occurs which is associated with the initial ohmic resistance of the system consisting of a membrane and a solution located between the ends of Lugin–Gabber capillaries. After this, a slow increase in the potential drop over time is observed which is associated with the decrease in the concentration of the electrolyte in the desalinated layer near the membrane. Further, the onset of a steady state is observed, at which the magnitude of the potential drop remains constant.

After 2.5 h of synthesis, the difference of potentials  $\Delta\phi$  in the system starts sharply increasing. This growth is possible in the case when the concentration of coun-

terions near the membrane surface becomes low in comparison with the concentration of ions in the bulk of the stirred solution and is observed in systems at currents above the limiting current. M.C. Martí-Calatayud et al. observed the presence of one more additional sharp growth in  $\Delta\phi$  in the ChP of a homogeneous membrane in a solution of  $\text{Fe}_2(\text{SO}_4)_3$  at currents above the limiting current which is determined by the formation of a layer of a  $\text{Fe}(\text{OH})_3$  deposit on the membrane [30]. In this case, the sharp growth in  $\Delta\phi$  after 2.5 h of synthesis is associated with the onset of formation of a dense layer of PANi, which has been confirmed by the data of optical microscopy (Fig. 4). Since the resistance of PANi is significantly higher than the resistance of the initial MK-40 membrane, the formation of its layer on the surface of the membrane leads to an increase in the value of  $\Delta\phi$ . After 10 min, the rate of growth in  $\Delta\phi$  decelerates, which evidences a rise of the conjugate effects of concentration polarization. In this case, this conjugate effect is water splitting on the membrane. Hydroxyl ions are transferred to the anode, which induces alkalization of the solution in the desalination compartment and a decrease in the rate of growth in  $\Delta\phi$  (Fig. 3).

The efficiency of surface modification of an MK-40 membrane with polyaniline has been confirmed by the data of optical microscopy. Insular character of the distribution of PANi can be observed on the surface of an MK-40 membrane (Fig. 4). It is seen in the images that the formation of PANi is only observed on the particles of the ion-exchange resin in an MK-40 membrane. An increase in the color intensity of the composites occurs with the increase in the time of synthesis of PANi, which indicates an increase in its amount in the samples.

After obtaining the composite membranes, the amount of aniline remaining in the solution feeding the desalination compartment was photometrically determined (Table 1). As it was expected, with increasing the time of synthesis, the amount of aniline in the solution decreases at a constant rate from the initial value of 0.01 down to 0.006 mol/L after 5 h of synthesis. A layer of PANi formed on the surface of the membrane which faces the concentration compart-

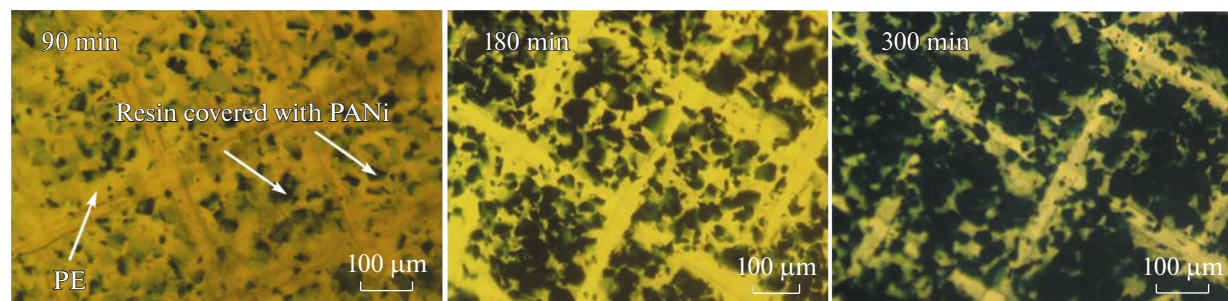


**Fig. 4.** Optical images of the surfaces of the composite membranes in the swelled state. The modification time is indicated in the image.

**Table 1.** Parameters of modification and properties of the membranes

Membrane	Modification time, min	Concentration of aniline in the desalination compartment after modification, mol/L	Thickness of the membranes, mm	Moisture content
MK-40	—	—	$0.51 \pm 0.01$	$0.42 \pm 0.02$
MK-40/PANi_1	90	0.009	$0.51 \pm 0.01$	$0.41 \pm 0.02$
MK-40/PANi_2	180	0.008	$0.54 \pm 0.01$	$0.40 \pm 0.02$
MK-40/PANi_3	300	0.006	$0.55 \pm 0.01$	$0.38 \pm 0.02$

ment does not prevent the passage of anilinium cations to the reaction zone.

The time required for visually uniform coloring of the entire working surface of the membrane with polyaniline is about 3 h. With the increase in the time of synthesis of PANi, the thickness of the sample increases, which confirms the formation of a noticeable amount of the modifier. In this case, a slight decrease in the moisture content of the modified membranes is observed, which should lead to some decrease in their thickness. However, the appearance of PANi compensates for this effect. The rate of the increase in the thickness of PANi layer on the surface of an MK-40 membrane has a nonmonotone character. After 1.5 h of synthesis, the thickness of the composite does not differ from that of the initial MK-40 membrane. However, after 3 h of synthesis, the thickness of the composite membrane increases by 6% in comparison with the initial membrane. These data also confirm the formation of a noticeable layer of PANi. After 5 h of synthesis, the thickness of the membrane slightly changes, which is associated with the decrease in its moisture content. Here, the amount of PANi continues increasing, which is seen by the image of the surface of the composite and decrease in the concentration of anilinium cations in the desalination compartment.

It is known that the moisture content of membranes depends on the nature and structure of the polymer matrix, amount of ionogenic groups in the membrane, and hydration capacity of the fixed groups and counterions. Since all the composites were obtained based on the same MK-40 membrane, the reason for the decrease in the moisture content is the appearance of PANi. N.P. Berezina et al. [31] found that intercalation of the aromatic chains of polyaniline into the membrane matrix induces reorganization of water molecules at the boundaries between the base polymer and electrically conductive chains of PANi.

Therefore, with the increase in the time of synthesis of PANi on the surface of an cation-exchange MK-40 membrane, the thickness of the obtained composite and uniformity of its coating with polyaniline increase and the moisture content decreases. This

is accompanied by a change in the electrochemical characteristics of the composite because water splitting at the depleted membrane/solution boundary starts at a current density below the limiting current density of the initial MK-40 membrane. After 2.5 h of synthesis, the layer of PANi uniformly and densely covers all the grains of the ion-exchange resin on the surface of the membrane.

#### *Voltammetry*

CVCs were measured for the initial and modified membranes in 0.05 mol-equiv/L solutions of NaCl (Figs. 5a, 5b), MgCl<sub>2</sub> (Figs. 5c, 5d), and CaCl<sub>2</sub> (Figs. 5e, 5f) in the case of orientation by the modified and unmodified layer to the counterion flow. The key characteristics of the current–voltage curve such as the values of the limiting and overlimiting current and values of the potential drop corresponding to them, slopes of the ohmic region, and plateau length were determined by the tangent method. The conductivity of the membranes was estimated from the slope of the ohmic region of the current–voltage curve.

#### *CVCs in the Case of Orientation of the Membrane by the Modified Layer to the Counterion Flow*

The synthesis of PANi on the surface of an cation-exchange MK-40 membrane for 90 min leads to an increase in the slope of the ohmic region in the CVC of the modified membrane by 30% in a solution of NaCl and by 20% in solutions of CaCl<sub>2</sub> and MgCl<sub>2</sub>, which suggests an increase in the conductivity of the system (Figs. 5a, 5c, 5e). After 180 min of synthesis, the slope of the ohmic region in the CVC of the modified membrane becomes comparable to that of the initial membrane in all the solutions under study (Figs. 5a, 5c, 5e). Further increasing the synthesis time of PANi leads to a decrease in the conductivity of the system in all the solutions under study. For an MK-40/PANi\_1 composite, an increase in  $i_{lim}$  by 17% relative to an MK-40 membrane is observed in a solution of NaCl and by 7% in solutions of CaCl<sub>2</sub> and MgCl<sub>2</sub>. Further increasing the time of synthesis time

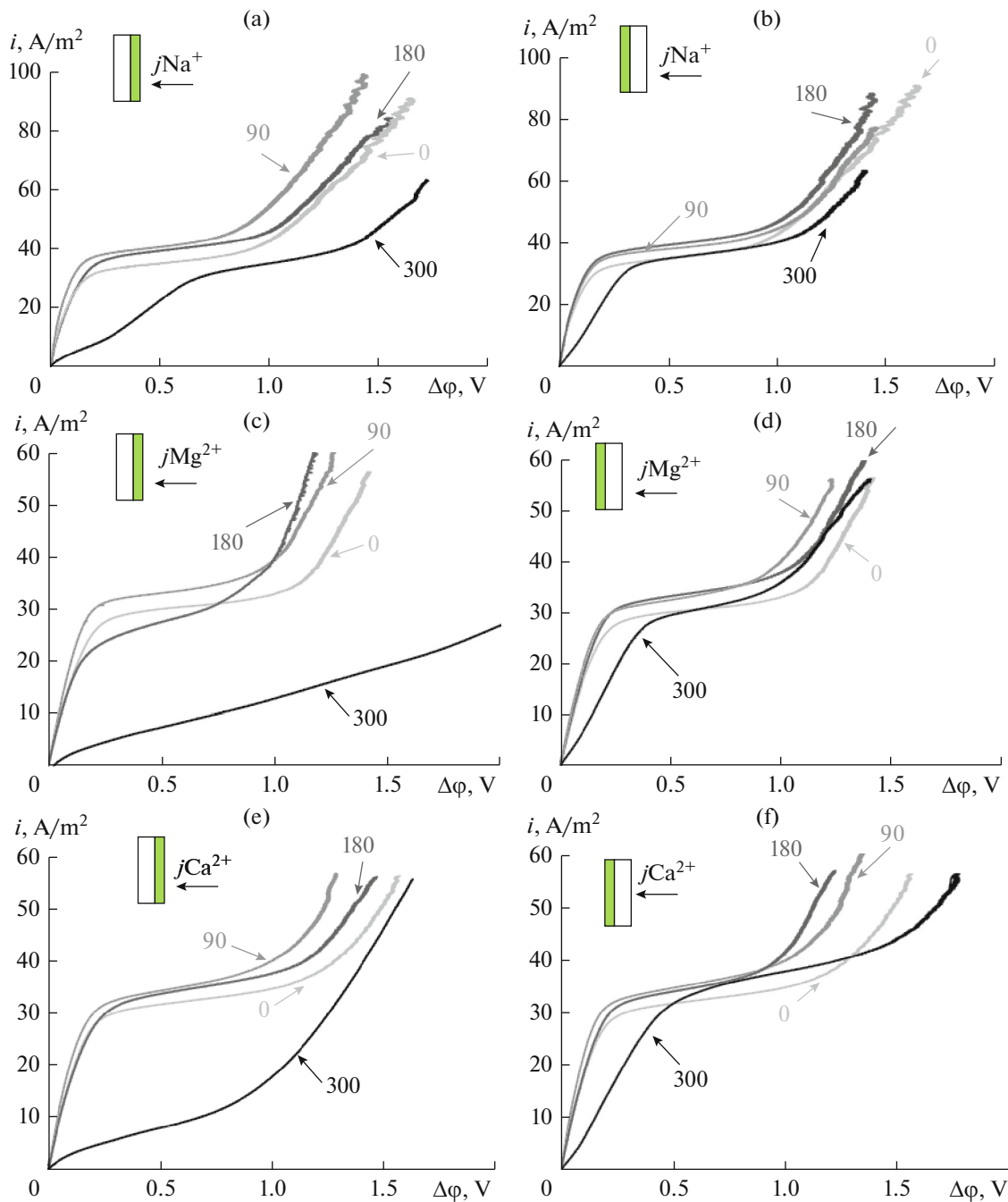


**Fig. 5.** CVCs of the initial and composite membranes in solutions of (a, b) NaCl, (c, d), MgCl<sub>2</sub>, and (e, f) CaCl<sub>2</sub> in the case of orientation by the (a, c, e) modified and (b, d, f) unmodified layer to the counterion flow. The numbers in the curves indicate the modification time of the sample in min.

of PANi on the surface of the membrane does not lead to an increase in  $i_{lim}$  but, on the contrary, leads to a decrease in this parameter. It should be noted that the value of  $i_{lim}$  on an MK-40/PANi\_2 membrane is by 13% higher in a solution of NaCl, comparable in a solution of CaCl<sub>2</sub>, and by 20% lower in a solution of MgCl<sub>2</sub> in comparison with an MK-40 membrane. The increase in the value of  $i_{lim}$  on an MK-40/PANi\_1

membrane as well as decrease in the resistance in the ohmic region of the CVC may be associated with the equilibrium electroconvection developing by the mechanism of 1st type electroosmosis because the concentration of the electrolyte near the membrane surface is relatively high at this time point, and no expanded space charge region is formed [32–34]. The boundary formed between the negatively charged

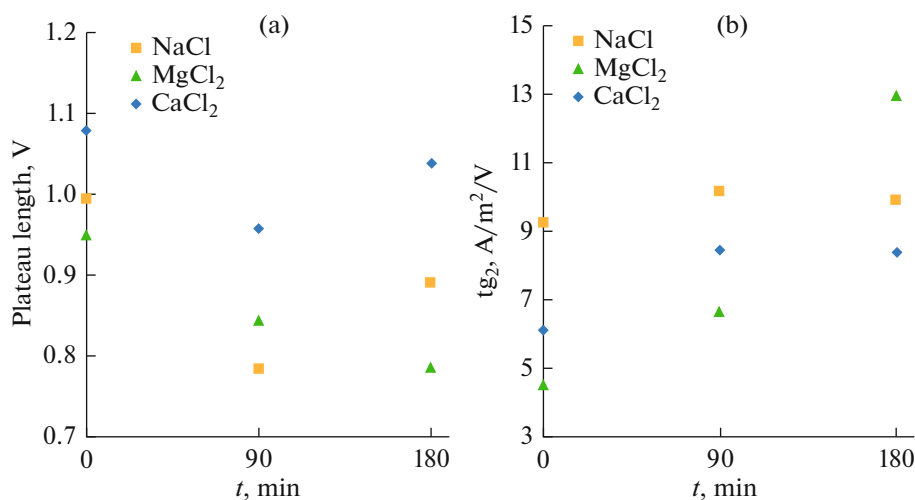


**Fig. 6.** Changes in the (a) length of the plateau and (b) its slope angle in the CVCs of the initial and composite membranes depending on modification time of the samples.

fixed groups of the ion-exchange resin and positively charged PANi determines the appearance of the tangential component of the electric force. The action of this force on the space charge region near the conductive surface induces formation of an electroconvective vortex. It is known that the properties of the surface of a membrane and distance between the conductive regions on the surface of a membrane substantially affect electroconvection [35]. As is seen from the data of optical microscopy (Fig. 4), the size of inclusions of PANi on the surface of an MK-40/PANi<sub>1</sub> membrane is much smaller, and the distance among them is much longer than on the surface of MK-40/PANi<sub>2</sub> and MK-40/PANi<sub>3</sub> membranes, which may lead to an increase in the number of electroconvective vortices per unit surface area. As a result, the value of the limiting current is higher in an MK-40/PANi<sub>1</sub> membrane than in an MK-40/PANi<sub>2</sub> membrane.

The changes in the plateau length  $\Delta$  depending on the time of synthesis of PANi in solutions of NaCl and CaCl<sub>2</sub> have an extreme dependence with the function minimum in the point corresponding to the time of modification of an MK-40/PANi<sub>1</sub> composite (Fig. 6a). In the case of a solution of MgCl<sub>2</sub>, the value of  $\Delta$  decreases with increasing the time of synthesis of PANi on the surface of an MK-40 membrane, which may be due to the precipitation and stronger water dissociation. Despite the fact that it was not possible to visualize the appearance of a precipitate on the membrane surface in a solution of magnesium chloride using optical microscopy, the presence of a small amount of precipitate is quite possible. Thus, in [36], the SEM method confirmed the formation of precipitates in a 0.04 M solution of magnesium chloride on the surface of an MK-40 membrane under similar experimental conditions.

The slopes of the plateau tg<sub>2</sub> for the modified MK-40/PANi<sub>1</sub> and MK-40/PANi<sub>2</sub> membranes are comparable between themselves and are higher in comparison with the initial membrane in solutions of NaCl and CaCl<sub>2</sub> (Figs. 6a, 6b). A different dependence is observed in a solution of MgCl<sub>2</sub>. The slope of the plateau increases in the series MK-40 < MK-40/PANi<sub>1</sub> < MK-40/PANi<sub>2</sub>. The reason for the change in the slope of the plateau is the nonuniformity of occurrence of the limiting state across the area of the membrane. Overlimiting transport is associated with the appearance of additional current carriers that appear due to the development of water splitting near the depleted membrane/solution boundary or conjugate convection [37, 38]. If no water splitting is observed at the membrane/solution interface, the decrease in the length of the plateau and increase in its slope can most likely be associated with the nonuniform development of nonequilibrium electroconvection near the membrane surface.

The CVC significantly transforms for the composite modified for 5 h. The amount of PANi and its uniform distribution on the membrane surface increase, and the modified layer with positively charged fixed groups increases the surface resistance of the membrane [39]. Two limiting currents are observed in the current–voltage curve of an MK-40/PANi<sub>3</sub> membrane (Fig. 5a) in a solution of NaCl. CVCs at different flow rates of the solution have been studied in detail for the obtained sample, which makes it possible to assess the contribution from the external and internal interfaces to the total effects of concentration polarization in all the solutions under study (Fig. 7). A constant value of the first limiting current in the region of low potentials and an expected increase in the second limiting current in the region of high potentials with the 1.5–3-fold increase in the flow rate of the



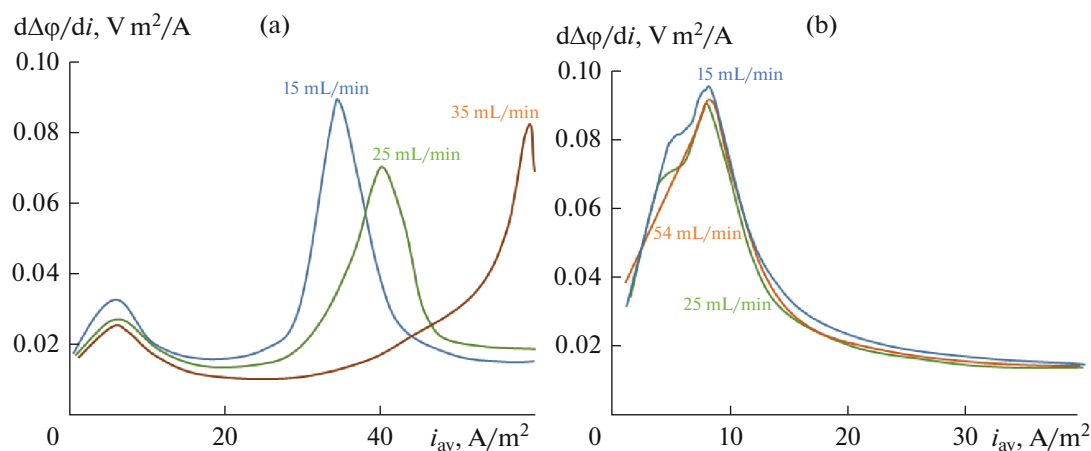


**Fig. 7.** Differential CVCs of an MK-40/PANi\_3 membrane in solutions of (a) NaCl and (b) CaCl<sub>2</sub> at different flow rates of the solution.

electrolyte have been found out in the differential CVC in a solution of NaCl (Fig. 7a). With the increase in the flow rate of the solution, the value of  $i_{lim}$  at the membrane/solution external boundary should increase due to the decrease in the thickness of the diffusion layer at the membrane/solution external interface. Because of this, the second limiting current in the differential curve has been called a “classical” limiting current induced by the decrease in the concentration of ions at the membrane/solution external interface like in the case of monopolar ion-exchange membranes. The first limiting current is “pseudolimiting” and refers to the depletion of the solution at the bipolar boundary inside the membrane. This bipolar boundary is formed in the process of preparation of the composite at the junction of the layer of PANi that possesses anion-exchange properties and an cation-exchange MK-40 membrane.

No classical limiting current is observed in the CVCs of an MK-40/PANi\_3 composite in solutions of CaCl<sub>2</sub> (Fig. 7b) and MgCl<sub>2</sub>, while the value of the pseudolimiting current remains unchanged with the increase in the flow rate of the solution.

#### *CVCs in the Case of Orientation of the Membrane by the Unmodified Surface to the Counterion Flow*

In the case of orientation of the composite by the unmodified side to the counterion flow in solutions of NaCl, MgCl<sub>2</sub>, and CaCl<sub>2</sub>, the conductivity of the system slightly changes for MK-40, MK-40/PANi\_1, and MK-40/PANi\_2 membranes, while the value of  $i_{lim}$  increases by 10% for MK-40/PANi\_1 and MK-40/PANi\_2 composites in comparison with the initial MK-40 membrane (Fig. 5). The decrease in the plateau length in the CVCs with increasing time of synthesis of PANi has been found in solutions of NaCl and MgCl<sub>2</sub>. However, the increase in the slope of the

plateau in the CVCs with increasing time of synthesis of PANi or modification time of the samples is only observed in solutions containing doubly charged cations. For an MK-40/PANi\_3 membrane, the value of  $i_{lim}$  becomes comparable to the initial membrane in solutions of NaCl and MgCl<sub>2</sub>, while it exceeds the value of  $i_{lim}$  for the initial membrane in a solution of CaCl<sub>2</sub>. However, the value of the potential drop, at which the limiting state appears, increases, and the conductivity of the system in the ohmic region of the CVCs becomes lower.

The clearly pronounced asymmetry of the parameters of the CVCs in solutions of NaCl, MgCl<sub>2</sub>, and CaCl<sub>2</sub> is only observed for the composite modified for 5 h (MK-40/PANi\_3). The comparison of the obtained CVCs (Fig. 5) and ChPs (Fig. 3) recorded in the process of synthesis of PANi on the surface of an MK-40 membrane makes it possible to suppose that the pronounced bipolar boundary between the layer of PANi and the initial membrane which leads to the asymmetry of the transport properties starts to form in the time period corresponding to the region of the ChPs, where decelerating growth in the potential drop accompanied by alkalization of the solution due to water splitting on the membrane is observed.

#### *Chronopotentiometry and Effect of pH*

To deeply study the development of effects associated with concentration polarization, ChPs of all the obtained membranes were measured in solutions of NaCl, CaCl<sub>2</sub>, and MgCl<sub>2</sub> with a concentration of 0.05 mol-equiv/L accompanied by the measurement of pH at the outlet from the desalination compartment. The value of pH in the desalination compartment depends on the difference between the flux of OH<sup>-</sup> ions generated on the membrane under study and flux of H<sup>+</sup> ions generated on the auxiliary anion-

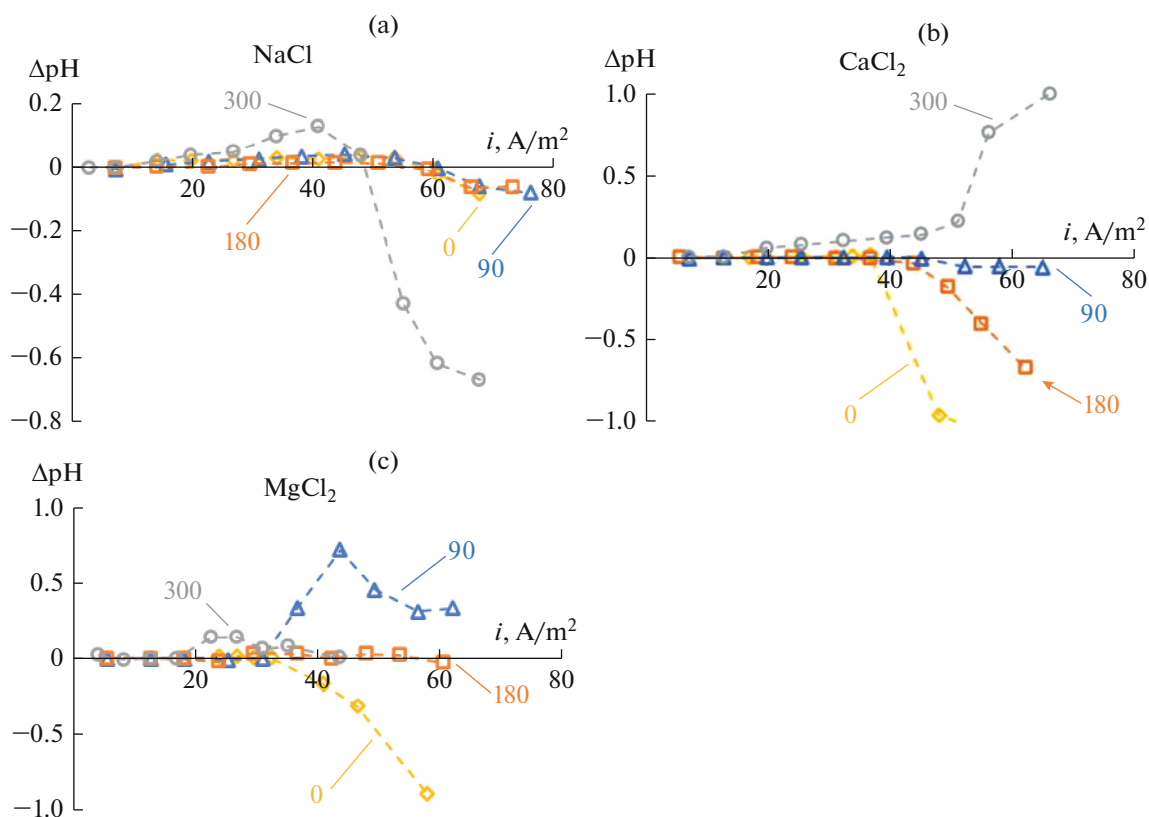


**Fig. 8.** Change in pH in the desalination compartment depending on the current density in the case of orientation of the composite by the modified side to the counterion flow. The numbers in the curves indicate the modification time of the sample in min.

exchange MA-40 membrane. When the flux of  $\text{OH}^-$  ions is higher than the flux of  $\text{H}^+$  ions, the solution in the desalination compartment is alkalinized. Otherwise, it is acidified. The recorded value of pH results from the process of water splitting on the anion- and cation-exchange membranes. However, since the same auxiliary MA-40 membrane is used in all the experiments, the analysis of the values of pH of the solution under desalination makes it possible to compare the rate of water splitting on different membranes under study at the same values of current density (Fig. 8).

In the underlimiting modes, no process of water splitting is observed on MK-40, MK-40/PANi<sub>1</sub>, and MK-40/PANi<sub>2</sub> membranes in all the solutions under study because the concentration of the ions of salts near the surface of the membrane is high. In a solution of NaCl, the process of water splitting at the depleted membrane/solution surface in the overlimiting current modes is the same for the MK-40, MK-40/PANi<sub>1</sub>, and MK-40/PANi<sub>2</sub> membranes (Fig. 8a). However, there is a different picture for an MK-40/PANi<sub>3</sub> membrane in the solution of NaCl. At current densities above  $20 \text{ A}/\text{m}^2$  ( $i/i_{\text{lim}} = 0.6$ ), slight alkalinization of the solution is noticeable in the desalination compartment. As it was shown above, there are two limiting currents in the CVC of such a composite. At a cur-

rent density of  $20 \text{ A}/\text{m}^2$  ( $i/i_{\text{lim}} = 0.6$ ), the classical limiting current density has not yet been reached; however, depletion of the solution of the electrolyte at the internal bipolar boundary between the layer of PANi and the membrane had already occurred, which had led to the water splitting at the internal boundary. Appearance of the first transition time can be observed in the differential ChP for an MK-40/PANi<sub>3</sub> membrane at  $i/i_{\text{lim}} = 0.6$  (Fig. 9a). Upon reaching the limiting current on an MK-40/PANi<sub>3</sub> membrane and up to  $i = 45 \text{ A}/\text{m}^2$  ( $i/i_{\text{lim}} = 1.5$ ), alkalinization of the solution continues in a solution of NaCl. Two transition times are observed in the differential ChP at these current modes (Fig. 9a), and the concentration of  $\text{OH}^-$  ions in the solution in the desalination compartment increases after the second transition time comes up. Therefore, the first transition time corresponds to the depletion of the internal bipolar boundary of an MK-40/PANi<sub>3</sub> membrane, and the second, to the depletion of the membrane/solution external boundary. Upon further increasing the current density, the water splitting on an anion-exchange MA-40 membrane develops stronger than on the membrane under study, because of which the solution in the desalination compartment is acidified.

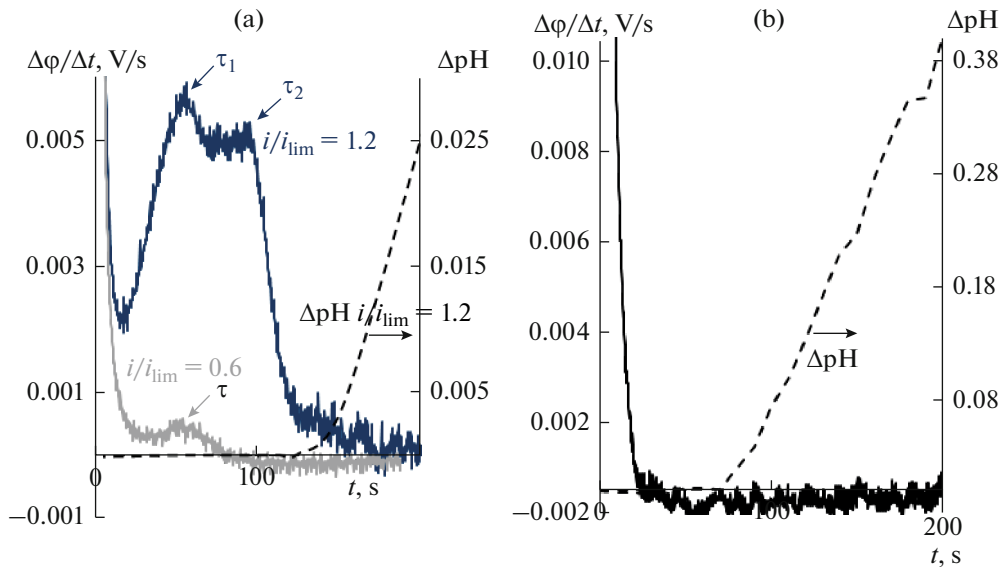


**Fig. 9.** Differential ChP for an MK-40/PANi\_3 membrane at (a)  $i/i_{\text{lim}} = 0.6$  and  $1.2$  in a solution of NaCl and (b)  $i = 56 \text{ A/m}^2$  in a solution of  $\text{CaCl}_2$  and corresponding to them changes in pH in the desalination compartment.

A solution of  $\text{CaCl}_2$  and  $\text{MgCl}_2$  in the desalination compartment starts being acidified at  $i = 40 \text{ A/m}^2$  ( $i/i_{\text{lim}} = 1.4$ ) on the initial MK-40 membrane (Figs. 8b, 8c). The water splitting on an anion-exchange MA-40 membrane develops stronger than on the MK-40 membrane under study because the ionogenic groups of an MA-40 membrane possess higher catalytic activity in the reaction of water splitting in comparison with the ionogenic groups of an MK-40 membrane [40]. Because of this, the solution in the desalination compartment is acidified. In the case of a solution of NaCl, the process of water splitting is not as strongly pronounced as in the solution with doubly charged ions. Water splitting sharply intensifies in this system upon replacing  $\text{Na}^+$  cations by  $\text{Ca}^{2+}$  and  $\text{Mg}^{2+}$  cations. The rate of water splitting on an MK-40/PANi\_1 membrane is higher than on an MK-40 membrane in solutions of  $\text{CaCl}_2$  and  $\text{MgCl}_2$  because the solution in the desalination compartment is slower acidified in an MK-40/PANi\_1//MA-40 system in comparison with an MK-40//MA-40 system. As it was expected, the rate of water splitting on the modified membranes is higher than on the initial MK-40 membrane in solutions of doubly charged ions. However, the rate of water splitting is lower on an MK-40/PANi\_2 membrane than on an MK-40/PANi\_1 membrane. Here, in the case of an MK-40/PANi\_3 membrane, the solution leaving the desalination compartment starts being alkalized already at  $i = 20 \text{ A/m}^2$  (Figs. 8b, 8c) in solutions of  $\text{CaCl}_2$  and  $\text{MgCl}_2$  as opposed to the membranes with a shorter modification time.

Strong water splitting at the internal bipolar boundary in  $\text{CaCl}_2$  and  $\text{MgCl}_2$  solutions leads to the appear-

ance of a flow of  $\text{OH}^-$  ions, which, in turn, can induce the exaltation effect [41]. The exaltation effect will not allow one to achieve a decrease in the electrolyte concentration in the diffusion layer, which corresponds to the onset of limit state at the outer boundary of the membrane/electrolyte solution. As is seen from the differential CVC (Fig. 7b), no limiting state occurs at the membrane/solution external boundary, which means that alkalization of the solution occurs due to the water splitting at the internal bipolar boundary. No transition time has been recorded in the differential ChP for an MK-40/PANi\_3 membrane in solutions of both  $\text{CaCl}_2$  (Fig. 9b) and  $\text{MgCl}_2$  even at relatively high current densities; however, here, quite intensive alkalization of the solution in the desalination compartment is observed. Upon further increasing the current density in a solution of  $\text{CaCl}_2$ , alkalization of the solution in the desalination compartment up to pH 7.5 is observed, while the value of pH does not exceed 6.5 in the region of current densities above  $i = 40 \text{ A/m}^2$  in a solution of  $\text{MgCl}_2$  (Figs. 8b, 8c). A deposit was found after the experiments in a solution of  $\text{MgCl}_2$  on an MK-40/PANi\_3 membrane (Fig. 10). The appearance of  $\text{OH}^-$  ions generated near the surface of an MK-40/PANi\_3 membrane//solution of  $\text{MgCl}_2$  leads to the formation of crystals of a deposit of  $\text{Mg}(\text{OH})_2$ , because of which, in this case, alkalization of the solution is not as noticeable as in the case with an MK-40/PANi\_3//solution of  $\text{CaCl}_2$  system. This is associated with the higher solubility of calcium hydroxide in comparison with magnesium hydroxide: the solubility product of  $\text{Mg}(\text{OH})_2$  at  $T = 25^\circ\text{C}$  is  $1.8 \times 10^{-11} \text{ mol}^3/\text{L}^3$ , while it is  $6 \times 10^{-6} \text{ mol}^3/\text{L}^3$  for  $\text{Ca}(\text{OH})_2$  [42].

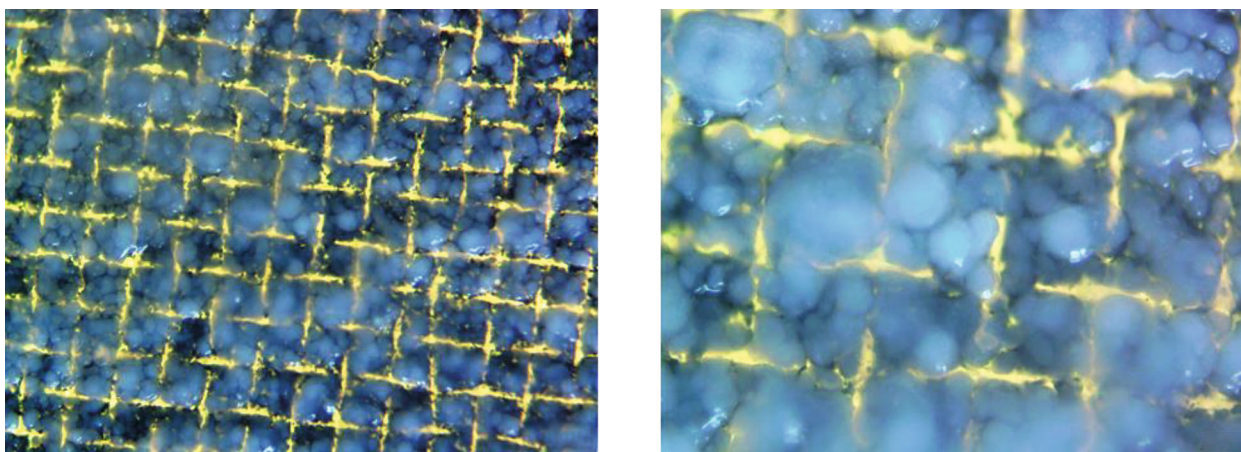


**Fig. 10.** Optical images of a deposit of  $\text{Mg}(\text{OH})_2$  on the surface of an MK-40/PANi\_3 membrane after the performed experiments in a solution of  $\text{MgCl}_2$ .

#### Transport Numbers of Counterions in the Membrane

To determine the transport numbers by chronopotentiometry by Eq. (2), it is necessary to know the apparent fraction of the conductive surface of the membrane  $\varepsilon$ . The apparent fraction of the conductive surface is calculated for all the membranes in a solution of  $\text{NaCl}$  and it is supposed that it remains unchanged in solutions of other electrolytes. The transition times are determined from the chronopotentiograms in the differential form, and the transport numbers of the cations in the membrane are determined by potentiometry by Eq. (3). The obtained value of  $\varepsilon$  is further used for the calculation of the transport numbers in solutions of  $\text{CaCl}_2$  and  $\text{MgCl}_2$ .

As is seen from Table 2, about 73% of the entire working surface of an MK-40 membrane is conductive. In the case of a small amount of PANi on the surface of an MK-40 membrane, the apparent fraction of the conductive surface grows for both orientations of the composite. Upon increasing the time of synthesis of PANi on the surface of the membrane (above 3 h), the apparent fraction of the conductive surface of the modified side of the membrane and transport number of  $\text{Na}^+$  ions in the membrane decrease.

After determining the apparent fraction of the conductive surface of the samples under study, the transport numbers of counterions in solutions of  $\text{CaCl}_2$  and

$\text{MgCl}_2$  are calculated. According to the data of a series of ChPs of the membranes under study, dependences of  $\tau$  on  $(C_0/i)^2$  are plotted for each individual solution (Fig. 11). The coefficient of the slope angle of the curve in the corresponding solution is used for the calculation of the transport number by Eq. (2) in solutions of  $\text{CaCl}_2$  and  $\text{MgCl}_2$ .

As is seen from Table 3, the transport number of the counterion in a cation-exchange MK-40 membrane decreases in a series  $\text{Na}^+$  (0.952) >  $\text{Mg}^{2+}$  (0.906) >  $\text{Ca}^{2+}$  (0.897). According to the data of Demina et al. [43], the amount of electrolyte sorbed by an MK-40 membrane increases upon the transition from singly to doubly charged counterion:  $\text{Na}^+ < \text{Mg}^{2+} < \text{Ca}^{2+}$ . The higher the Donnan sorption the higher the number of coions present in the membrane and the lower its selectivity. The adequacy of determination of the TNs by chronopotentiometry for the initial MK-40 membrane makes it possible to apply this method for the assessment of the selectivity of the obtained composite membranes.

An increase in the transport numbers of  $\text{Mg}^{2+}$  and  $\text{Ca}^{2+}$  is observed for the membranes with the time of modification with PANi of less than 3 h (Table 3). No appearance of a transition time in a solution of  $\text{CaCl}_2$  has been recorded in the chronopotentiograms of an MK-40/PANi\_3 composite in the case of orientation

**Table 2.** Transport numbers of  $\text{Na}^+$  ions and apparent fraction of the conductive surface of the membranes at different orientations of the membranes to the counterion flow

Membrane	$i_i^{\text{app}}$ (mod. side)	$i_i^{\text{app}}$ (unmod. side)	$\varepsilon$ (mod. side)	$\varepsilon$ (unmod. side)
MK-40	0.952 ± 0.017		0.729 ± 0.025	
MK-40/PANi_1	0.957 ± 0.013	0.965 ± 0.015	0.907 ± 0.023	0.941 ± 0.024
MK-40/PANi_2	0.937 ± 0.014	0.941 ± 0.016	0.921 ± 0.023	0.935 ± 0.023
MK-40/PANi_3	0.863 ± 0.015	0.885 ± 0.012	0.685 ± 0.017	0.836 ± 0.021

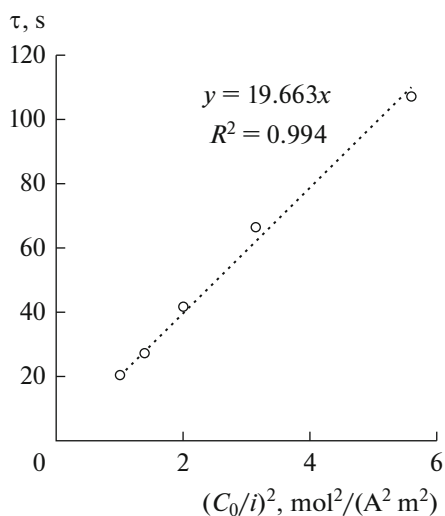


**Fig. 11.** Dependence of  $\tau$  on  $C_0/i$  obtained for an MK-40 membrane in 0.05 M NaCl for the determination of the apparent fraction of the conductive surface.

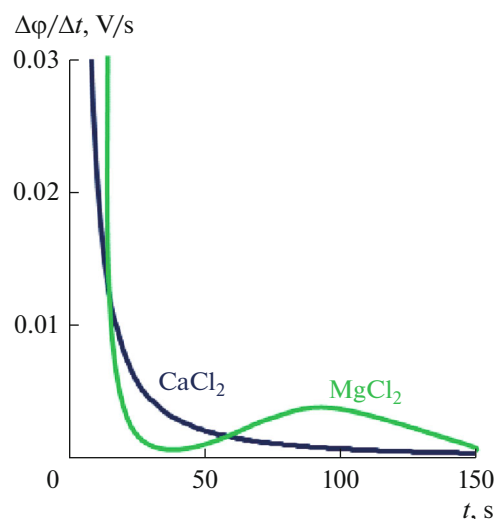


**Fig. 12.** Differential ChP for an MK-40/PANi\_3 membrane by the modified side to the counterion flow at  $i = 42 \text{ A/m}^2$  in solutions of  $\text{CaCl}_2$  and  $\text{MgCl}_2$ . The membrane is in a horizontal position.

by the modified side to the counterion flow (Fig. 12). Because of this, it appears impossible to calculate the transport numbers of  $\text{Ca}^{2+}$  cations. The chronopotentiograms of an MK-40/PANi\_3 composite in a solution of  $\text{MgCl}_2$  have the same shape as in a solution of  $\text{CaCl}_2$ . However, the local maximum is present in differential ChP (Fig. 12) which may be associated with the appearance of a deposit of  $\text{Mg}(\text{OH})_2$  on the membrane surface (Fig. 10).

Increasing the time of synthesis of PANi on the surface of an ion-exchange membrane up to 3 h leads to a decrease in the transport numbers of singly charged cations and an increase in the transport numbers of doubly charged cations. However, upon further increasing the time of synthesis of PANi, samples with a clearly pronounced bipolar boundary formed at the junction of the ion-exchange resin and polyaniline are obtained. The transport numbers of singly charged cations in such a composite membrane decrease. Hydrogen and hydroxyl ions formed at the space charge regions at the internal bipolar boundary are involved in the process of ion transport through the composite membrane in solutions with doubly charged cations.  $\text{H}^+$  and  $\text{OH}^-$  ions prevent the transfer of doubly charged ions through the membrane to a

greater extent than of the singly charged  $\text{Na}^+$  ion. Here, according to the Donnan effect, the application of a positively charged layer onto the surface of a cation-exchange membrane leads to electrostatic repulsion of cations moving across the field through the membrane. Ions with a higher charge repulse from the surface of a composite membrane with a greater force than in the case of singly charged ions. It can be assumed that the formation of a dense layer of PANi on the surface of membranes also leads to a decrease in the sizes of the surface defects at the junction between the grain of the ion-exchange resin and polyethylene. Here, a sieve effect can appear which will promote transport of ions with a smaller radius in the hydrated state.

## CONCLUSIONS

A series of composite ion-exchange membranes based on an heterogeneous cation-exchange MK-40 membrane and polyaniline has been obtained. An increase in the intensity of coloration of the composites and their thickness is observed with the increase in the time of synthesis of polyaniline, which indicates an

**Table 3.** Transport numbers of the cations in the membrane at different orientations of the membranes to the counterion flow

Membrane	$\bar{t}_{\text{Ca}^{2+}}$ (mod. side)	$\bar{t}_{\text{Ca}^{2+}}$ (unmod. side)	$\bar{t}_{\text{Mg}^{2+}}$ (mod. side)	$\bar{t}_{\text{Mg}^{2+}}$ (unmod. side)
MK-40	$0.897 \pm 0.034$		$0.906 \pm 0.034$	
MK-40/PANi_1	$0.967 \pm 0.025$	$0.970 \pm 0.025$	$0.939 \pm 0.025$	$0.976 \pm 0.025$
MK-40/PANi_2	$0.965 \pm 0.024$	$0.975 \pm 0.025$	$0.955 \pm 0.024$	$0.965 \pm 0.024$
MK-40/PANi_3	—	$0.971 \pm 0.025$	—	$0.971 \pm 0.025$

increase in the amount of polyaniline in the samples. The synthesis process of polyaniline on the surface of the membrane was accompanied by the recording of chronopotentiograms and pH of the solution leaving the desalination compartment, which made it possible to determine the time required for obtaining a sample with a dense layer of polyaniline which was at least 3 h. At this particular time, a sharp potential drop is observed in the chronopotentiogram which is determined by the appearance of a significant layer of polyaniline which possesses higher resistance in comparison with the initial MK-40 membrane. Increasing the time of modification of the membrane leads to the appearance of a water splitting at the membrane/solution interface in the underlimiting current mode, which suggests a change in the electrochemical properties of the composite.

The initial cation-exchange MK-40 membrane and composites obtained based on it have been studied by voltammetry and chronopotentiometry in solutions of NaCl, CaCl<sub>2</sub>, and MgCl<sub>2</sub> in the same flow-type electro dialysis cell, in which the samples were obtained. For the sample modified for 1.5 h, an increase in the conductivity and value of the limiting current in the solutions under study in comparison with the initial membrane has been found in the case of its orientation by the modified side to the counterion flow. The changes in the parameters of the current–voltage curve of the composites in overlimiting current modes are associated with the development of water splitting at the depleted membrane/solution boundary which intensifies with the increase in the time of synthesis of polyaniline. The presence of two limiting currents has been for the first time found for a composite obtained based on a heterogeneous membrane, and the time of synthesis of polyaniline required for obtaining a composite with the clearly pronounced asymmetry of the transport properties has been found to be 5 h. Two limiting currents are observed in the current–voltage curve in the case of orientation of an MK-40/PANi<sub>3</sub> composite by the modified side to the counterion flow in a solution of NaCl. It has been shown that the first pseudolimiting current is determined by the depletion of the internal bipolar boundary formed between the layer of polyaniline possessing weak anion-exchange properties and the cation-exchange membrane. The second limiting current is a classical limiting current induced by the depletion of the concentration of ions on the membrane/solution external interface. It has been found that the current–voltage curves of such a composite depend on the nature of the electrolyte. Appearance of only a pseudolimiting current associated with the increase in the rate of water splitting at the internal bipolar boundary in comparison with a solution of NaCl is observed in the current–voltage curve of an MK-40/PANi<sub>3</sub> composite in solutions of CaCl<sub>2</sub> and MgCl<sub>2</sub> in the case of orientation by the modified side to the counterion flow.

The transport numbers of counterions in the initial membrane and composites based on it have been determined by chronopotentiometry. Increasing the time of synthesis of polyaniline on the surface of an ion-exchange membrane up to 3 h leads to a decrease in the transport numbers of singly charged cations and an increase in the transport numbers of doubly charged cations. However, upon further increasing the modification time, due to the formation of a clearly pronounced bipolar boundary in the membrane, the hydrogen and hydroxyl ions appearing on it are predominantly transported through the membrane, to a greater extent preventing the passage of doubly charged Ca<sup>2+</sup> and Mg<sup>2+</sup> ions than Na<sup>+</sup> ions, which makes the prepared samples promising for application in the processes of electro dialysis separation of singly and doubly charged ions.

#### FUNDING

The study was supported by Russian Science Foundation, grant no. 22-29-00938, <https://rscf.ru/project/22-29-00938/>.

#### CONFLICT OF INTEREST

The authors declare that they have no conflicts of interest.

#### REFERENCES

1. M. Yaqub, M. N. Nguyen, and W. Lee, *Sci. Total Environ.* **844**, 157081 (2022).
2. N. Mir and Y. Bicer, *J. Environ. Manage.* **289**, 112496 (2021).
3. A. S. Stillwell and M. E. Webber, *Water* **8**, 601 (2016).
4. S. Al-Amshawee, M. Y. B. M. Yunus, A. A. M. Azodein, D. G. Hassell, I. H. Dakhil, and H. A. Hasan, *Chem. Eng. J.* **380**, 122231 (2020).
5. E. O. Ezugbe and S. Rathilal, *Membranes* **10**, 89 (2020).
6. Y. Oren, E. Korngold, N. Daltrophe, R. Messalem, Y. Volkman, L. Aronov, M. Weismann, N. Bouriakov, P. Glueckstern, and J. Gilrona, *Desalination* **261**, 321 (2010).
7. Y. Zhang, K. Ghyselbrecht, R. Vanherpe, B. Meesschaert, L. Pinoy, and B. Van der Bruggen, *J. Environ. Manage.* **107**, 28 (2012).
8. A. Subramani and J. G. Jacangelo, *Sep. Purif. Technol.* **122**, 472 (2014).
9. C. Jiang, Y. Wang, Z. Zhang, and T. Xu, *J. Membr. Sci.* **450**, 323 (2014).
10. L. Ge, B. Wu, D. Yu, A. N. Mondal, L. Hou, N. U. Afsar, Q. Li, T. Xu, J. Miao, and T. Xu, *Chin. J. Chem. Eng.* **25**, 1606 (2017).
11. T. Sata, *J. Polym. Sci. Polym. Chem. Ed.* **16**, 1063 (1978).
12. J. Ying, Y. Lin, Y. Zhang, Y. Jin, H. Matsuyama, and J. Yu, *Chem. Eng. J.* **446**, 137076 (2022).
13. J. Pan, L. Zhao, X. Yu, J. Dong, L. Liu, X. Zhao, and L. Liu, *Chin. Chem. Lett.* **33**, 2757 (2022).

14. X. Pang, Y. Tao, Y. Xu, J. Pan, J. Shen, and C. Gao, *J. Membr. Sci.* **595**, 117544 (2020).
15. M. Vasselbehagh, H. Karkhanechi, R. Takagi, and H. Matsuyama, *J. Membr. Sci.* **490**, 301 (2015).
16. X. Pang, X. Yu, Y. He, S. Dong, X. Zhao, J. Pan, Zh. Runnan, and Liu L, *Sep. Purif. Technol.* **270**, 118768 (2021).
17. V. Compana, E. Riande, F. J. Fernandez-Carretero, N. P. Berezina, and A. A.-R. Sytcheva, *J. Membr. Sci.* **318**, 255 (2008).
18. M. Kumar, M. A. Khan, Z. A. A. Othman, and M. R. Siddiqui, *Desalination* **325**, 95 (2013).
19. H. Farrokhzad, S. Darvishmanesh, G. Genduso, T. Van Gerven, and B. Van der Bruggen, *Electrochim. Acta* **158**, 64 (2015).
20. T. Luo, S. Abdu, and M. Wessling, *J. Membr. Sci.* **555**, 429 (2018).
21. E. Stránská, *Desalin. Water Treat.* **56**, 3220 (2015).
22. N. A. Kononenko, O. A. Demina, N. V. Loza, S. V. Dolgoplov, and S. V. Timofeev, *Rus. J. Electrochem.* **57**, 505 (2021).
23. K. S. Barros, M. C. Martí-Calatayud, T. Scarazzato, A. M. Bernardes, D. C. R. Espinosa, and V. Pérez-Herranz, *Adv. Colloid. Interface* **293**, 102439 (2021).
24. J.-H. Choi and S.-H. Moon, *J. Membr. Sci.* **191**, 255 (2001).
25. S. A. Mareev, V. S. Nichka, D. Y. Butylskii, M. K. Urtenov, N. D. Pismenskaya, P. Y. Apel, and V. V. Nikonenko, *J. Phys. Chem.* **120**, 13113.
26. V. I. Zabolotskii, N. P. Berezina, V. V. Nikonenko, V. A. Shaposhnik, and A. A. Tskhai, *Membrany* **4**, 6 (1999).
27. M. Andreeva, N. Loza, N. Kutenko, and N. Kononenko, *J. Solid State Electrochem.* **24**, 101 (2020).
28. N. V. Loza, I. V. Falina, N. A. Kononenko, and D. S. Kudashova, *Synth. Met.* **261**, 116292 (2020).
29. R. A. Robinson and R. H. Stocks, *Electrolyte Solutions* (Dover Publications, New York, 2002).
30. M. C. Martí-Calatayud, M. García-Gabaldón, and V. Pérez-Herranz, *J. Membr. Sci.* **443**, 181 (2013).
31. N. P. Berezina, A. A. Kubaisy, S. V. Timofeev, and L. Karpenko, *J. Solid State Electrochem.* **11**, 378 (2007).
32. I. Rubinstein and B. Zaltzman, *Phys. Rev. Lett.* **114**, 114502 (2015).
33. I. Rubinstein and B. Zaltzman, *Phys. Rev. Fluids*, 093702 (2017).
34. V. V. Nikonenko, S. A. Mareev, N. D. Pis'menskaya, A. V. Kovalenko, M. K. Urtenov, A. M. Uzdenova, and G. Pourcelly, *Rus. J. Electrochem.* **53**, 1122 (2017).
35. S. Zyryanova, S. Mareev, V. Gil, E. Korzhova, N. Pismenskaya, V. Sarapulova, O. Rybalkina, E. Boyko, Ch. Larchet, D. Lasaad, and V. Nikonenko, *Int. J. Mol. Sci.* **21**, 973 (2020).
36. M. A. Andreeva, V. V. Gil, N. D. Pismenskaya, V. V. Nikonenko, L. Dammak, C. Larchet, D. Grande, and N. A. Kononenko, *J. Membr. Sci.* **540**, 183 (2017).
37. A. Campione, L. Gurreri, M. Ciofalo, G. Micale, A. Tamburini, and A. Cipollina, *Desalination* **434**, 121 (2018).
38. N. D. Pismenskaya, V. V. Nikonenko, E. I. Belova, G. Yu. Lopatkova, Ph. Sstat, G. Pourcelly, and K. Larshe, *Rus. J. Electrochem.* **43**, 307 (2007).
39. X. Pang, Y. Tao, Y. Xu, J. Pan, J. Shen, and C. Gao, *J. Membr. Sci.* **595**, 117544 (2020).
40. V. I. Zabolotskii, N. V. Shel'deshov, and N. P. Gnusin, *Russ. Chem. Rev.* **57**, 801 (1988).
41. Yu. I. Kharkats // *Elektrokhimiya*. 1985. V. 21. P. 974.
42. L. G. Sillen and A. E. Martell, *Stability Constants of Metal-Ion Complexes* (Chemical Society, London, 1964).
43. O. A. Demina, I. V. Falina, N. A. Kononenko, and V. I. Zabolotskiy, *Colloid J.* **82**, 108 (2020).

*Translated by E. Boltukhina*